Commissioning and optimization of superconducting undulator in the horizontal state

Zilin Chen,[†] Xiangchen Yang, Xiangzhen Zhang,[‡] Junhao Wei,[†] Xiaojuan Bian, Jieru Geng,[‡] Yao Gao, and Yuhui Li[*]

Institute of High Energy Physics, Chinese Academy of Sciences, Beijing 100049, China

(Received 30 November 2023; accepted 5 February 2024; published 21 February 2024)

Taking advantage of a higher field than a conventional permanent magnet undulator, superconducting undulators (SCUs) have been rapidly developed in recent years for applications at synchrotron radiation sources and free-electron lasers. The Institute of High Energy Physics, Chinese Academy of Sciences, has developed a 1.5-m long planar SCU with a short period of 15 mm. This SCU has been commissioned and optimized in the horizontal position. In contrast to the vertical position, where the undulator coils are immersed in liquid helium for superconductivity, the horizontal test requires the assembly of the complete device, including the cryostat, current conductor, cryocooler, vacuum chamber, and undulator coils. This test reflects the operation status and measures the SCU's characteristics under working conditions. Although experiences from the vertical test provided good guidance for horizontal optimization, special care needs to be taken for effects such as gravity. After improving field uniformity through iterative measurements, the rms phase error of the SCU is reduced to 7.3° at a current of 400 A. Additionally, the functions of the end correction coils to mitigate field integral errors have been verified. This paper also demonstrates and analyzes other phenomena and interesting observations during the commissioning process. It discusses important issues that impact field quality and measurement accuracy and suggests further improvement measures for an even better field.

DOI: 10.1103/PhysRevAccelBeams.27.022401

I. INTRODUCTION

In recent years, there has been an increasing demand for synchrotron radiation performance. Thanks to the efforts of major laboratories, conventional permanent magnet (PM) undulators (cryogenic permanent magnet undulator, in-vacuum undulator, etc.) have achieved excellent results but are gradually approaching their physical limits [1–3]. It has been reported that superconducting undulators (SCUs) have gradually become new research hotspot because SCUs can obtain higher peak magnetic fields than cryogenic permanent magnet undulators and in-vacuum undulators for the same period length (λ_u) and magnetic gap (g) [4,5]. The SCU can simply change the magnetic field amplitude by varying the working current to meet the users' needs, avoiding the need for expensive precision motion equipment. Superconducting magnets are insensitive to radiation under the protection of a vacuum chamber (VC) and are not easily demagnetized under irradiation like the PM undulator [6]. Therefore, SCUs have a very promising future for advanced photon sources such as diffraction limited storage rings and free-electron lasers (FELs) [7–9].

There are also many difficulties in the development of SCUs, such as winding magnets with superconducting wires, quench protection, and cryostat support. In order to protect the magnet and reduce the gas load of ultrahigh vacuum during accelerator operation, a beam vacuum chamber must exist inside the magnetic gap, which occupies the space of the magnetic gap, resulting in the inability of the SCU to achieve the same gap as the PM undulator at the same physical aperture of the beam. For the SCU, the peak magnetic field B_0 on the center axis of the magnetic gap can be expressed as

$$B_0 = \sum_{n=1,3,5,\ldots} \left[\frac{4\mu_0}{n^2\pi} \frac{j}{k_u} \sin\left(\frac{nk_u a}{2}\right) e^{-\frac{nk_u g}{2}} (1 - e^{-nk_u b}) \right], \quad (1)$$

where $k_u = \frac{2\pi}{\lambda_u}$, j is the current density, and a,b are the cross-sectional dimensions of the coils. The increase in g

[*]Corresponding author: liyuhui@ihep.ac.cn
Also at University of Chinese Academy of Sciences, Beijing 100049, China.
[†]Also at China Spallation Neutron Source, Institute of High Energy Physics, Chinese Academy of Sciences, Dongguan 523000, China.
[‡]Also at University of Chinese Academy of Sciences, Beijing 100049, China.

TABLE I. Parameters of the SCU developed by IHEP.

Parameter	Attribute or value
Core and pole material	DT4
Superconducting wire material	NbTi/Cu
Period length (mm)	15
Number of periods	100
Pole width (mm)	3
Wire slot width (mm)	4.5
Good field width in x direction[a] (mm)	± 12
Gap (mm)	9.5
Peak field (T)	>0.5

[a]Def. Good field: $|(B_y|_{x=\pm 12} - B_y|_{x=0})|/(B_y|_{x=0}) < 0.5\%$.

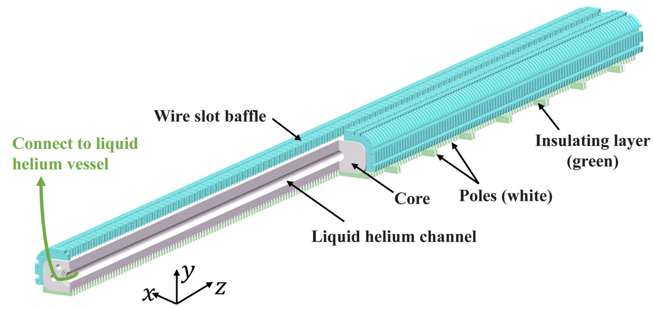

FIG. 2. Construction diagram of one part of SCU magnet.

requires the SCU to have a higher working current to achieve the desired magnetic field. The only institutions that have achieved long-term stable operation of SCUs on accelerators are the Institute for Beam Physics and Technology at the Karlsruhe Institute of Technology with the synchrotron KARA and Argonne National Laboratory with APS-U [10–12].

Since 2020, the Institute of High Energy Physics of the Chinese Academy of Sciences (IHEP, CAS) has initiated the development of SCUs, with the first phase being the development of a 1.5-m long planar SCU based on NbTi wire with the parameters shown in Table I. Previously, the 1.5-m long SCU has completed magnetic field measurements and online correction in a liquid-helium Dewar in the vertical state [13]. In this paper, we will present our efforts in the past year for the commissioning and optimization of the 1.5-m long SCU in the horizontal state and summarize the experience gained in the SCU development process as well as our outlook for the future.

II. ASSEMBLY AND ALIGNMENT OF SCU IN THE HORIZONTAL STATE

The SCU is in the horizontal state, i.e., its working state on the accelerator, suspended in a cryostat by thermally insulated carbon fiber rods, as shown in Fig. 1. The SCU operates in a significantly different environment in the horizontal state compared to in the vertical state. At first, the SCU works conduction cooled in the horizontal state rather than being directly immersed in liquid helium as in the vertical state. The cryocoolers condense helium gas to liquid helium, which flows through the channel inside the core which is made from a single block of pure iron in Fig. 2 to cool the coils to 4.2 K to reach the superconducting state. Second, the SCU is stressed significantly differently in the horizontal state than in the vertical state. In the horizontal state, the SCU's own gravity acts in the direction of the magnetic gap (y direction), which makes the gap more difficult to constrain and may cause changes in the magnetic field. Third, the SCU must be equipped with a beam vacuum chamber in operating condition. There are two reasons for this. One is related to the cooling method of the cryostat. The cooling refrigeration efficiency of conduction cooling is much lower than that of liquid-helium immersion. In order to reduce the efficiency of heat radiation from the high-temperature environment to the cryogenic magnet, it is necessary to wrap enough adiabatic materials on the surface of the magnet. These adiabatic

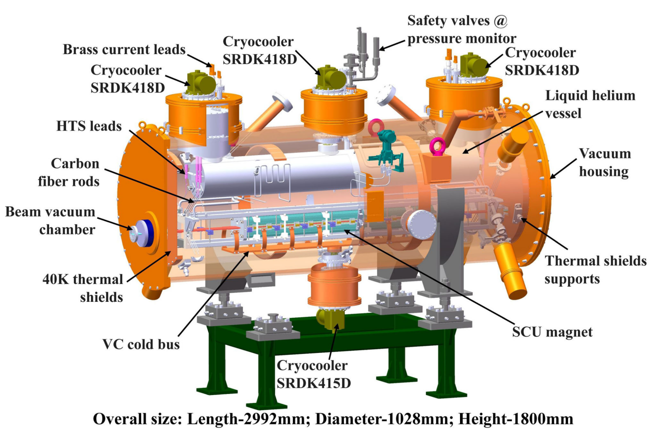

FIG. 1. 3D view of the SCU magnet and cryostat assembly in the horizontal state.

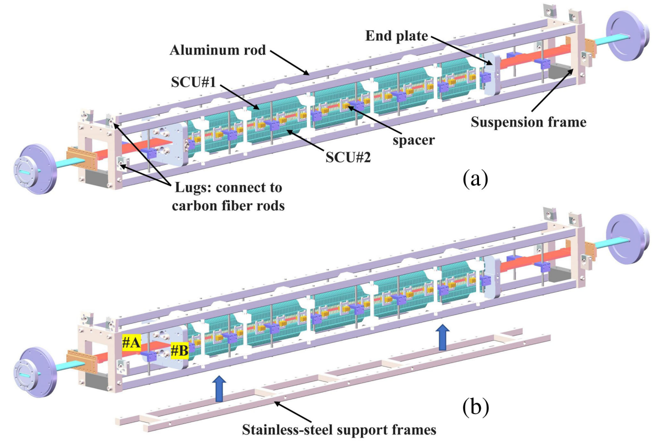

FIG. 3. Schematic of the SCU magnet and beam vacuum chamber being secured to the cage: (a) the original design of the cage without additional support; (b) a set of stainless-steel support frames were added to increase the rigidity of the cage.

(a)

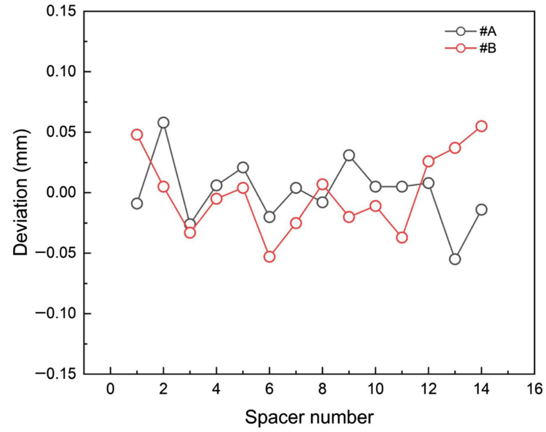

(b)

FIG. 4. Horizontal state of the SCU magnet obtained by the laser tracker: (a) photograph of the process of collimating the SCU; (b) trend of SCU deviation from the horizontal line.

materials are porous materials with huge outgassing, making it difficult to achieve ultrahigh vacuum. Therefore, it is necessary to build an ultrahigh vacuum environment for the operation of the beam in the magnetic gap separately. Second, the beam passing through the components will induce image currents on the surface, in order to prevent the image currents from directly acting on the superconducting magnet to make the SCU quench, a vacuum chamber is needed to realize rf shielding.

In order for the SCU to be suspended in the cryostat, a suitable "cage" was designed and machined. At the initial stage, the cage consists of four long aluminum rods with good thermal conductivity and two end suspension frames, as shown in Fig. 3(a), with the magnet connected to the cage as a whole through the end plates. The lugs on the suspension frame will be lifted by carbon fiber rods at the appropriate position, and the position of the magnet in the cryostat will be adjusted by adjusting the tension of the rods. During actual assembly, the aluminum rods were not as stiff as expected, causing the magnet and cage to sag severely under the influence of gravity. A set of stainless-steel support frames can resist this deformation, as shown in Fig. 3(b). Due to the different shrinkage coefficients of aluminum and stainless steel, it is important to provide a reasonable gap for the difference in shrinkage between the two during assembly. The spacers used to determine the magnetic gap are among the most precisely machined parts in the SCU, so the position of the spacers can be used to determine whether the SCU is horizontal or not. As in Fig. 4(a), the suspension frames at each end of the cage are supported to simulate its state in a cryostat, and the horizontality of the magnetic center can be determined by tracing the undulation of the line connected by the spacers relative to the horizontal line with a laser tracker. As shown in Fig. 4(b), the overall deviation of the spacers on both sides of the SCU is less than 0.06 mm, and the maximum deflection deformation of 0.05 mm for a single SCU magnet is counteracted by the support of the cage, which meets the engineering requirements. The vacuum chamber is centered on the magnetic gap by determining the distance between its outer wall surface and the magnet by means of a feeler gauge. The SCU magnet is carefully wrapped in multilayer insulation (MLI) and then fed into the cryostat for integration as shown in Fig. 5, including electrical connections such as current leads, wires of quench protection monitoring and temperature sensors, positioning of the magnet centers and beam trajectories in the cryostat, connection of liquid helium piping, and sealing for ultrahigh vacuum.

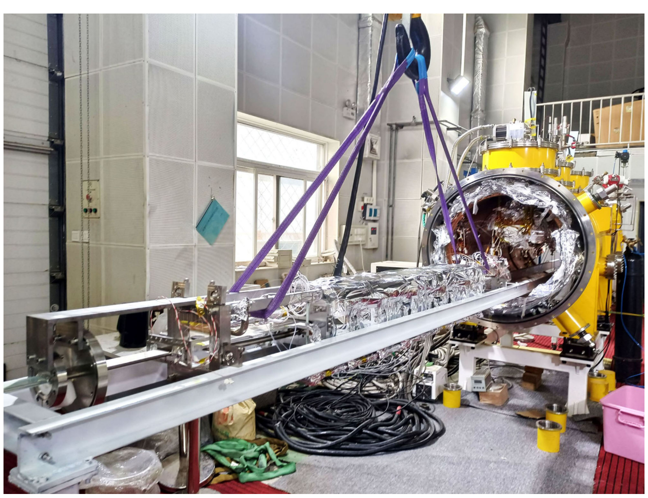

FIG. 5. Photo of the SCU magnet with wrapped multilayer insulation (MLI) entering the cryostat.

III. TEST RESULTS AND OPTIMIZATION

The SCU magnet reached 4.2 K in about 7 days under the action of the cryocoolers, as shown in Fig. 6. SCU 1 and SCU 2 underwent separation and reassembly from the vertical state to the horizontal state. From the process of training in Fig. 7, the memory effect of the superconducting coils was significantly altered. Together with the limitation

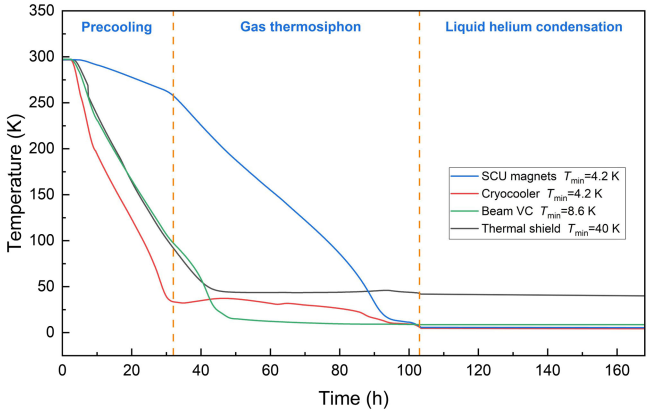

FIG. 6. Cooling process of the conduction-cooled SCU in the cryostat.

of the cooling efficiency of the cryostat, the SCU's working current reached 420 A after about 50 quenches in the first quench training in the cryostat, which was much less efficient than the training in the vertical state. In the horizontal state, the SCU magnet accomplished two fine adjustments of the magnetic gap, and their overall force state did not change significantly, so the training efficiency was significantly improved.

Measuring the magnetic field of the SCU in the horizontal state uses the same motion mechanism as in the vertical state. The motor-driven ultralong stroke bellows drive the Hall probe to scan the magnetic field in the magnetic gap, as in Fig. 8, where the beam vacuum chamber serves as a track for the "sled" instead of the guide rails in the vertical state. As in the vertical state, some collimating structures are used to maintain the straightness of the motion mechanism, and the magnetic field is scanned to record data when the sled is pulled. The sled carrying the Hall probe is rigorously manufactured to ensure that the center of the Hall probe is centered on the x and y direction of the sled. The sled slides in the vacuum chamber that is precisely positioned during the SCU assembly process. All Computer Numerical Control (CNC) machining and assembly errors are required to be controlled within 0.01 mm. The trajectory scanned by the Hall probe is thus the magnetic axis as well as the beam trajectory. The motor is also collimated by laser trackers and has a separate encoder that records the position of the Hall probe and sends trigger signals to the voltmeter to record the Hall probe's voltage signals. The model of the Hall probe used is LakeShore's HGCT-3020 (InAs Hall Sensor). Each Hall probe was calibrated at room temperature and tested for temperature dependent sensitivity. Measurements were temperature compensated according to the ambient temperature of the vacuum chamber in which the Hall probe was located, with a measurement error of no more than 0.5%. Figure 9 shows the magnetic field distribution along the z axis at the center of the magnetic gap at 400 A measured during a recent SCU training, characterizing the magnetic field measurement system in normal working condition.

The magnetic gap and assembly method for the first training of the SCU in the horizontal state is based on the correction results in the vertical state. After scanning the magnetic field, however, a significant raised trend in the peak magnetic field was found, as shown in Fig. 10 (red line), which is important evidence of the effect of the change in the force state of the SCU magnet on the magnetic field distribution. Accordingly, the root-mean-square (rms) phase errors of the SCU deteriorate from 4.2° (200 A), 6.4° (300 A), and 8.2° (400 A) in the vertical state to 7.3° (200 A), 12.0° (300 A), and 18.5° (400 A), which is unacceptable for an insert device operating on an accelerator [14,15]. In the vertical state, we can easily obtain the amount of adjustment to the magnetic gap to flatten the amplitude of the peak magnetic field as a whole through the variation of Eq. (1), i.e.,

$$g = -\frac{2}{k_u}\ln\left(\frac{\pi}{4\mu_0}\frac{k_u}{j}\frac{1}{\sin(\frac{k_u a}{2})(1-e^{-k_u b})}\frac{B_y(z)}{\sin(k_u z)}\right), \tag{2}$$

$$\Delta g = -\frac{2}{k_u}\ln\left(\frac{B_y(z)+\Delta B}{B_y(z)}\right), \tag{3}$$

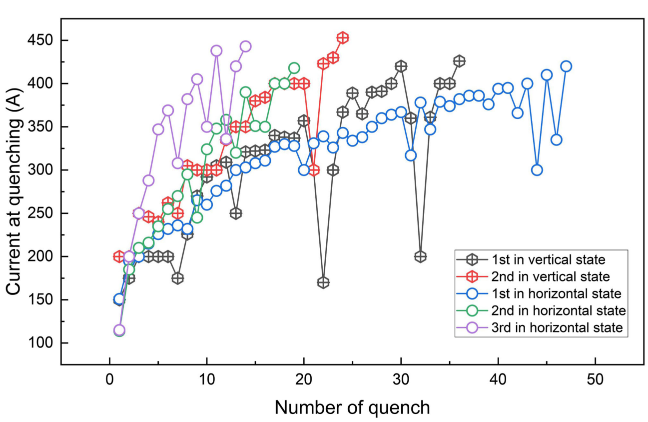

FIG. 7. Quench training process of SCU in different states.

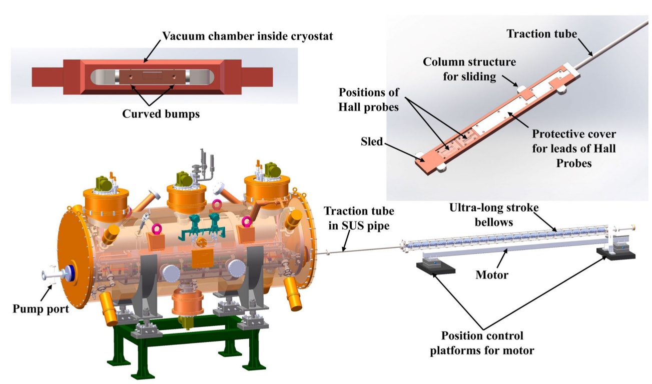

FIG. 8. 3D schematic of the device for scanning the SCU 's magnetic field in the horizontal state.

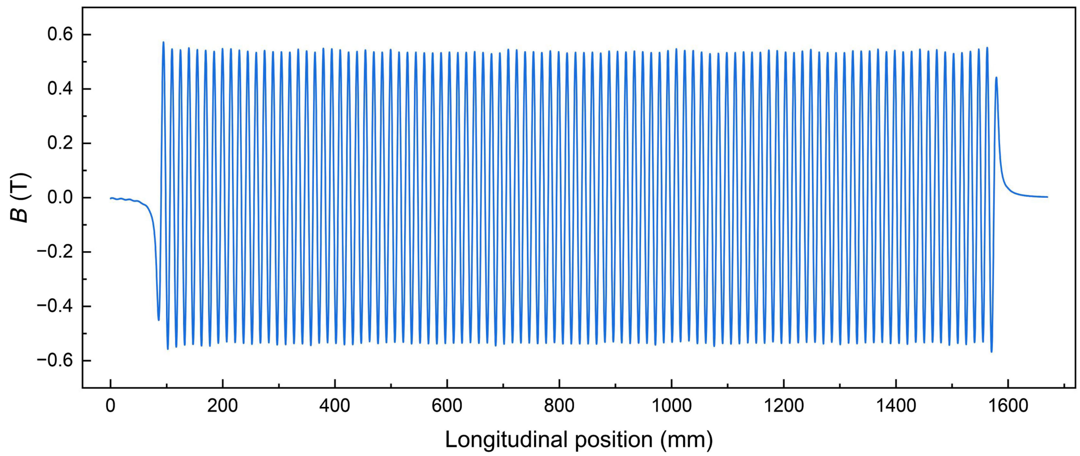

FIG. 9. The magnetic field distribution of the SCU (400 A) obtained from the Hall probe scan.

where $B_y(z)$ is the magnetic field data along the z axis at the center of the magnetic gap scanned by the Hall probe and ΔB is the expected magnetic field adjustment amount. According to Eq. (3), several pairs of thickened spacers were replaced for the SCU in the horizontal state at the location of the peak magnetic field raise. The peak magnetic field obtained again showed a depressed distribution as in Fig. 10 (blue line). Obviously, under the influence of gravity, adjusting the magnetic gap exactly according to Eq. (3) is unreliable.

Nevertheless, Eq. (3) can still provide a theoretical guide for adjusting the magnetic field, and one of our experiences, combined with the experimental results, is to determine the adjustment of the magnetic gap to be half of the result of Eq. (3). The SCU with reworked spacers was trained again and the magnetic field was measured. The peak magnetic field distributions obtained at currents of 200, 300, 350, 400, and 420 A are shown in Fig. 11, and the overall dispersion of the peak magnetic field (in terms of standard deviation) has been reduced by 49% and 22%, respectively, compared to the previous two measurements. The peak magnetic field optimized for the SCU in the horizontal state is compared with the peak magnetic field in the vertical state, as shown in Fig. 12 for 350 A. The peak magnetic fields in the two states are not exactly coincident due to changes in the state of force and magnetic gap. However, it is interesting to note that the trend of the peak magnetic field at most of the poles is the same, which indicates that the magnetic field distribution of the SCU is still reproducible after many rounds of optimization, and the adjustment of the magnetic gap does not affect the magnetization effect inside the magnet. It should be noted that the SCU in the horizontal state has a tendency to have a high peak magnetic field at several poles at the front end. This is due to the fact that the ends of the SCU are firmly fixed to the end plates, and it is difficult to forcefully correct the magnetic field by changing the thickness of the spacers, which reminds us to change the fixation of the ends to

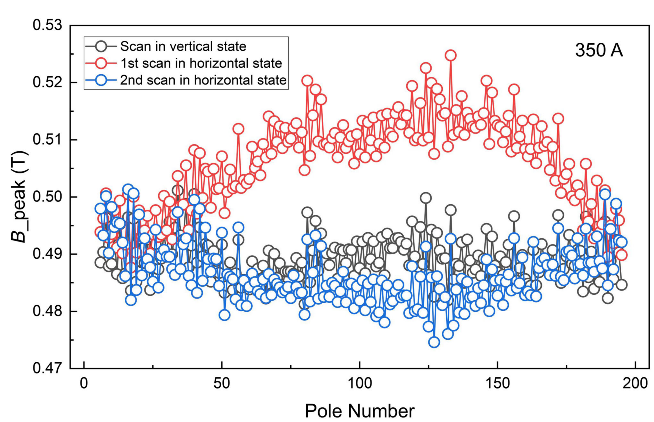

FIG. 10. Comparison of the peak magnetic field of the SCU as affected by gravity (blue line) and the peak field corrected only by the equation (red line) with the peak field in the vertical state (black line).

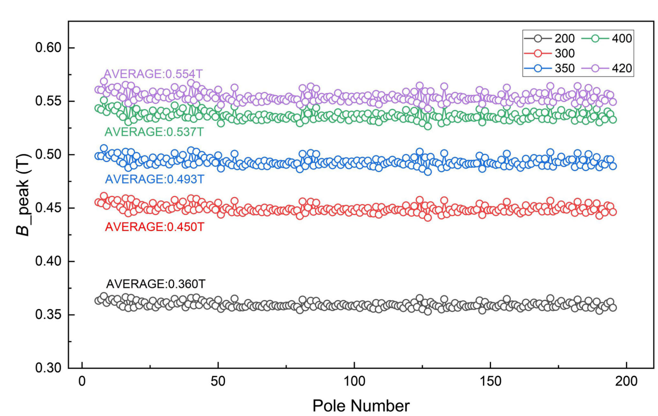

FIG. 11. Peak magnetic field of the SCU for each working current optimized by combining theoretical equations and experience.

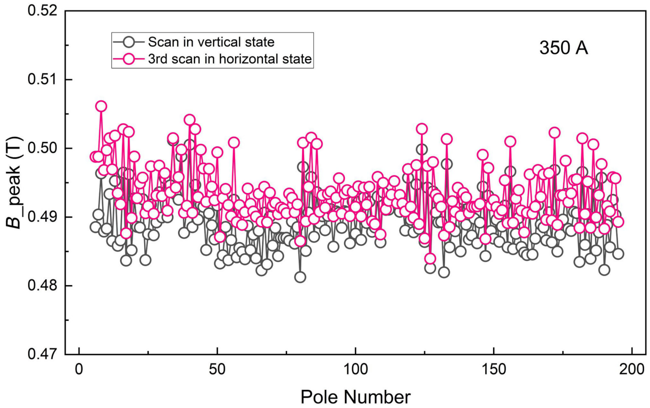

FIG. 12. Peak magnetic field of the optimized SCU in the horizontal state compared to the vertical state.

provide a means for magnetic field optimization in the future manufacturing of SCUs. With the magnetic field distribution, we can easily calculate the phase error. As in Fig. 13, the pole-by-pole phase error distribution at each current is shown and the rms phase error can be obtained. The rms phase errors at 200, 300, and 400 A are 3.4°, 6.0° and 7.3°, respectively, which are even better than that of the SCU in the vertical state.

The uniformity of the peak magnetic field is a visual representation of the quality of the SCU's magnetic field, and the phase error is an important parameter that responds to the photon intensity of the radiation produced by the SCU. In addition to this, we need to consider the effect of the magnetic field on the beam. For an ideal planar SCU with only a vertically oriented magnetic field (B_y), the motion of the beam at the center of the magnetic gap follows

$$x'' = \frac{d^2x}{dz^2} = -\frac{eB_y}{\gamma m_0 v_z}, \tag{4}$$

where γ is the Lorentz Factor, m_0 is the electron static mass, and v_z is the longitudinal velocity of the beam. When the beam enters the SCU with an initial deflection angle of 0, its angular deflection $x'(z)$ and transverse displacement $x(z)$ at any position on the z axis are

$$x'(z) = -\frac{e}{\gamma m_0 v_z}\int_0^z B_y(z_1)dz_1 = -\frac{e}{\gamma m_0 v_z} I_1(z), \tag{5}$$

$$x(z) = -\frac{e}{\gamma m_0 v_z}\int_0^z I_1 dz_2 = -\frac{e}{\gamma m_0 v_z} I_2(z), \tag{6}$$

where I_1 is the first integral of the magnetic field and I_2 is the second integral of the magnetic field. I_1 and I_2 are proportional to the angular deflection and displacement of the beam, respectively. In order to minimize the effect of SCU on the beam, the magnetic field integral needs to be minimized. For planar SCUs, additional winding of the correction coils at the end optimizes the integral of the magnetic field, especially the second integral of the magnetic field, which strongly depends on the end field [16].

As in Fig. 14, the 1.5-m long SCU is wound with a set of correction coils in the first two wire slots near the end. The total number of coil turns in each wire slot is 72, with 59

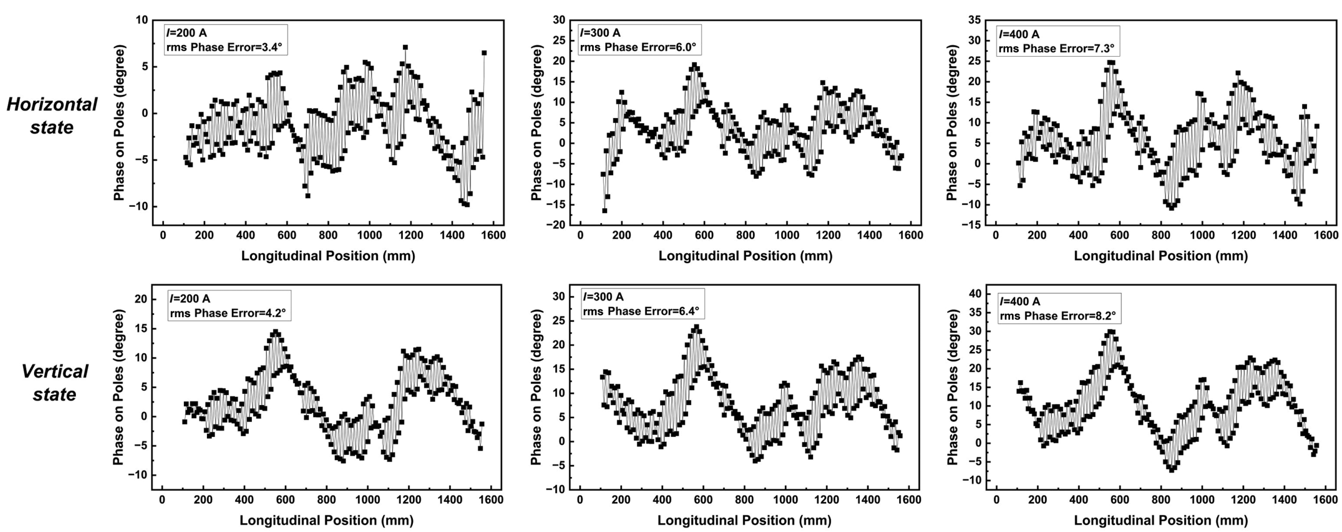

FIG. 13. Phase error of the optimized SCU in the horizontal state at each working current.

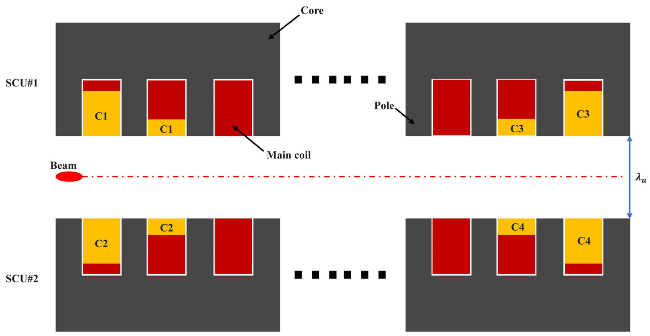

FIG. 14. Design of the correction coils at the ends of the 1.5-m long SCU.

turns of correction coils in the first wire slot, 20 turns of correction coils in the second wire slot, and the rest as main coils. In each slot, the correction coils and the main coils are wound in the same direction. The two sets of correction coils, C1 and C2, are connected in series and energized by a power supply independent of the main coils, as is the case at the other end of the SCU. The integral of the magnetic field is corrected by adjusting the positive, negative, and magnitude of the correction currents during the magnetic measurement. Figure 15 shows the process of finding an appropriate correction current at the main coil current of 400 A. The desired correction can be obtained by integrating the magnetic field secondarily at 400 A without correction current. The horizontal coordinate is the longitudinal length of the SCU, and the vertical coordinate is the difference between the amount of correction desired at that position with the amount of correction provided by the correction coils, i.e., ΔC. A positive ΔC means that the $I_2(z)$ is undercorrected, and a negative ΔC means that the $I_2(z)$ is overcorrected. With a main coil current of 400 A, a correction current of 11.5 A provides the most appropriate amount of correction. At this correction current, we also obtained the smallest rms phase error of 7.3°.

IV. DISCUSSION

The development of the 1.5-m long SCU underwent several vertical and horizontal commission and optimization. Some of the problems and phenomena encountered are the experiences we have gained and the direction we will strive for in our future work.

In the vertical state, we had expected that in addition to training the SCU, it would be possible to optimize the SCU's magnetic field in a simple mode that did not break electrical connections in order to reduce the work in the horizontal state. Because of the space constraints of the cryostat, all types of wiring have to be reconnected and SCU magnet needs to be recollimated for each optimization in the horizontal state. Unfortunately, we underestimated the effect of gravity on the SCU. Still, the experience of optimization in the vertical state helped us to obtain a better-quality magnetic field in the horizontal state. Although this process is very complex, it is necessary for the SCU that is to run on an accelerator. When longer or other types of SCUs are wound next, more robust fixed structures will be used to assemble the SCUs to counteract the effects of gravity on the magnetic field.

Oscillations of the peak magnetic field around the mean value were observed in the magnetic field measurements in both the vertical and horizontal states, as shown in Fig. 12. The fact that the oscillations have the same trend at each pole indicates that the oscillations are uncorrelated with the magnetic gap and that the oscillations originate from within the magnet. Measurement of the residual magnetism of the SCU after training with a current of 400 A revealed that the magnitude of the residual magnetism at each pole was not uniform. Moreover, after applying current in the reverse direction, the direction of the residual magnetism was also reversed, but the magnitude was not the same as that of the residual magnetism after training with forward current. This indicates that the cores are not uniformly magnetized or there are mechanical errors in the assembly of the cores

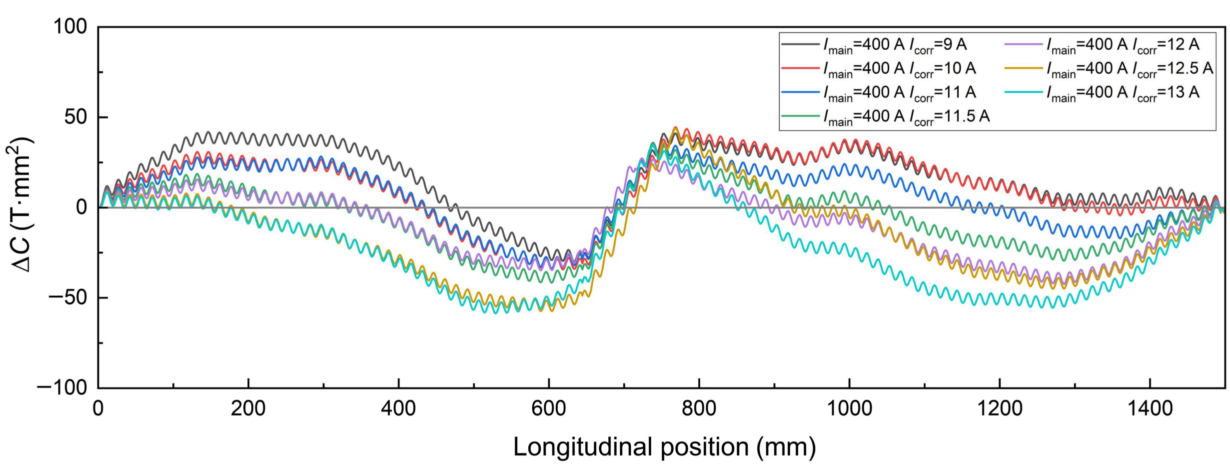

FIG. 15. The ability of different correction currents to correct the second integral of the magnetic field of the 1.5-m long SCU.

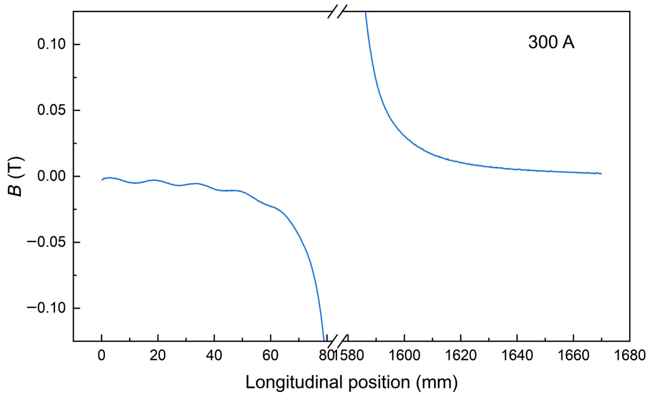

FIG. 16. Undulations observed during the initial stage of scanning the magnetic field.

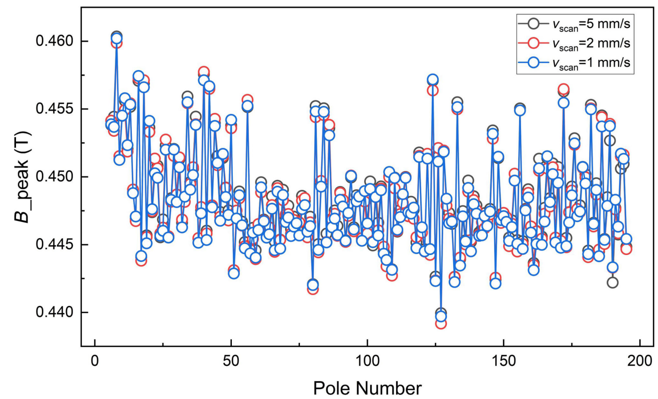

FIG. 18. Comparison of peak magnetic fields obtained by scanning at different speeds.

and poles, which results in oscillations in the peak magnetic field. Therefore, materials with better mechanical and magnetic properties than DT4 should be selected as the cores for the next SCU manufacturing, and the cores and poles should be processed in an integrated manner instead of being assembled after separate processing as at present.

During the magnetic field measurements, we found undulations of the magnetic field at the initial position but not at the end, as shown in Fig. 16. This asymmetrical result is clearly not the actual magnetic field and is presumably caused by eddy currents in the copper sled. The sled has to be long enough to store the leads of the Hall probe, so in Fig. 8, the Hall probe is positioned at the end of the sled. At the start of the scan, the majority of the sled senses the magnetic field before the Hall probe, and the magnetic flux changes to create eddy currents. The effects caused by eddy currents are greater than the magnetic field at the location of the Hall probe thus creating undulations. In the end, the eddy currents caused by the change in magnetic flux had essentially no effect on the Hall probe at the high magnetic field, so no undulation was observed. Since the length of the sled is designed to be an integral multiple of the SCU's period length, the sled is essentially free of eddy currents in the magnetic gap. Scanning the magnetic field at different speeds confirmed the presence of eddy currents, as shown in Fig. 17. However, the peak magnetic field obtained at different speeds was nearly unchanged, as shown in Fig. 18, and the rms phase errors did not differ by more than 0.1°, indicating that the presence of eddy currents had a limited effect on the magnetic field measurements. Since the magnetic measuring equipment currently used is inside a vacuum at low temperatures, it is necessary to use a rigid metal as a Hall probe's carrier to ensure safety. The planned magnetic field measurement system in air is being developed as shown in Fig. 19. An adiabatic guide tube is inserted into the beam vacuum chamber, and the Hall probe's carrier is dragged through the tube by wrapping mechanisms at the ends of the cryostat. The Hall probe's carrier can be made entirely of nonmetallic materials to eliminate the effects of eddy currents.

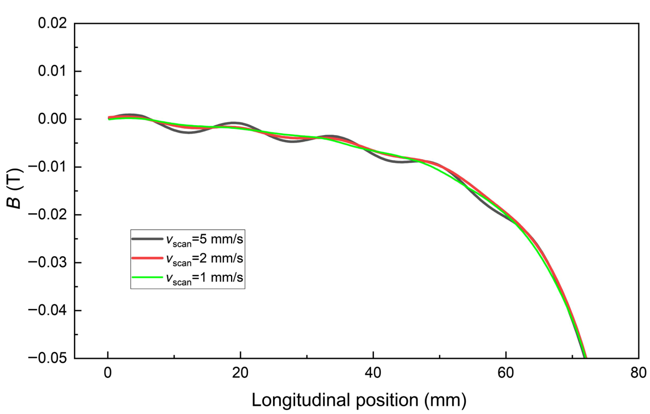

FIG. 17. Magnetic field profiles at the initial position obtained by scanning at different speeds.

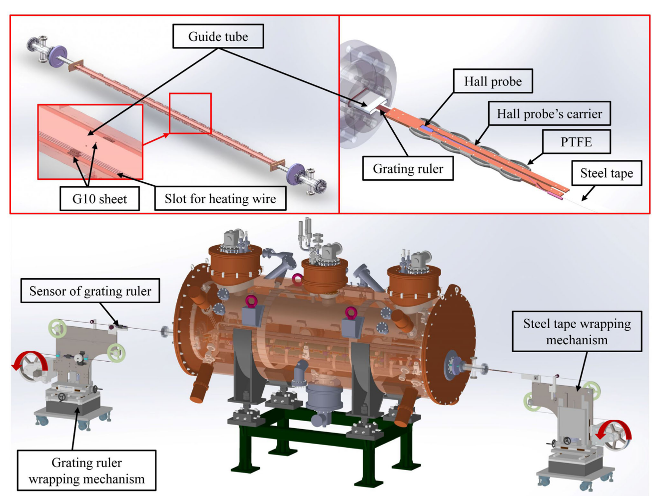

FIG. 19. 3D schematic of the measurement system in air planned to be built for scanning the SCU magnetic field.

V. CONCLUSION

IHEP has achieved milestones in the development of the SCU. The 1.5-m long SCU was commissioned and optimized in a cryostat in the horizontal state.

The 1.5-m long SCU was reassembled from the vertical to the horizontal state so that the memory effect of the superconducting coils has been reduced. The SCU was retrained in the cryostat and the maximum main coil current is now almost close to the current in the vertical state. Under the influence of gravity, the magnetic field of the SCU in the horizontal state has changed, mainly in the uneven peak magnetic field and worse phase error. The method of optimizing the magnetic field in the vertical state has helped us to recorrect the magnetic field of the SCU and optimize it further, but the effect of the force on the magnet also needs to be considered in the process. Currently, the rms phase error of the 1.5-m long SCU is controlled within 10° for the range of main coils currents that can be achieved. In addition, the ability of the correction coils at the end to correct the second integral of the magnetic field is verified. By scanning the magnetic field after applying the currents of different correction coils at the same main coils current, the corresponding optimal correction current values can be obtained to provide a reference when the SCU is operated in an accelerator in the future.

Some of the problems that arose during the commissioning process are discussed and analyzed. Accordingly, the optimization schemes that need to be adopted in the future when developing new SCUs are proposed. Stronger supports will be used to minimize the effect of gravity on the magnetic field. The selection of better ferromagnetic materials and more precise manufacturing methods reduce the dispersion of the peak magnetic field. The development of a more convenient magnetic field measurement system will allow for smaller errors in magnetic field measurements.

Next, IHEP plans to develop more types of SCUs, including planar SCUs with shorter period lengths and smaller magnetic gaps, polarization-adjustable SCUs, period-length-variable SCUs, and high-temperature superconducting undulator. We expect that SCUs can make excellent contributions to future advanced synchrotron radiation sources and FELs.

ACKNOWLEDGMENTS

The relevant work presented in this paper is supported by the funding number "E029A5M111" of CAS and "No. 12205318" of the National Natural Science Foundation of China. We also appreciate the help of Engineers Lingling Men and Xiaoyang Liu of IHEP in the collimation.

[1] C. Benabderrahmane, P. Berteaud, M. Valléau, C. Kitegi, K. Tavakoli, N. Béchu, A. Mary, J. Filhol, and M. Couprie, Nd2Fe14B and Pr2Fe14B magnets characterisation and modelling for cryogenic permanent magnet undulator applications, Nucl. Instrum. Methods Phys. Res., Sect. A **669**, 1 (2012).

[2] M. Musardo, O. Chubar, T. Tanabe, J. Rank, A. Banerjee, T. Corwin, D. Harde, C. Eng, and C. Kitegi, Design, construction, and magnetic field characterization of a segmented adaptive-gap in-vacuum undulator prototype for NSLS-II, J. Phys. **2380**, 012015 (2022).

[3] J. Bahrdt and E. Gluskin, Cryogenic permanent magnet and superconducting undulators, Nucl. Instrum. Methods Phys. Res., Sect. A **907**, 149 (2018).

[4] E. Moog, R. J. Dejus, and S. Sasaki, Comparison of achievable magnetic fields with superconducting and cryogenic permanent magnet undulators—a comprehensive study of computed and measured values (2017), https://doi.org/10.2172/1372292.

[5] P. Emma, N. Holtkamp, H. Nuhn, D. Arbelaez, J. Corlett, S. Myers, S. Prestemon, R. Schlueter, C. Doose, J. Fuerst, Q. Hasse, Y. Ivanyushenkov, M. Kasa, G. Pile, E. Trakhtenberg, and E. Gluskin, A plan for the development of superconducting undulator prototypes for LCLS-II and future FELs, in *Proceedings of FEL2014, Basel, Switzerland* (2014), https://escholarship.org/uc/item/5hs0h07j.

[6] T. Bizen, R. Kinjo, T. Hasegawa, A. Kagamihata, Y. Kida, T. Seike, T. Watanabe, T. Hara, T. Itoga, Y. Asano, and T. Tanaka, Radiation-induced magnetization reversal causing a large flux loss in undulator permanent magnets, Sci. Rep. **6**, 37937 (2016).

[7] K. Zhang and M. Calvi, Review and prospects of worldwide superconducting undulator development for synchrotrons and FELs, Supercond. Sci. Technol. **35**, 093001 (2022).

[8] J. Feldhaus and B. Sonntag, *Strong Field Laser Physics*, Springer Series in Optical Sciences (Springer, New York, 2008), pp. 91–107.

[9] A. Ghaith, M.-E. Couprie, D. Oumbarek-Espinos, I. Andriyash, F. Massimo, J. Clarke, M. Courthold, V. Bayliss, A. Bernhard, M. Trunk, M. Valléau, O. Marcouillé, A. Chancé, S. Licciardi, V. Malka, F. Nguyen, and G. Dattoli, Undulator design for a laser-plasma-based free-electron-laser, Phys. Rep. **937**, 1 (2021).

[10] S. Casalbuoni, A. Cecilia, S. Gerstl, N. Glamann, A. Grau, T. Holubek, C. Meuter, D. S. de Jauregui, R. Voutta, C. Boffo, T. Gerhard, M. Turenne, and W. Walter, Overview of the superconducting undulator development program at ANKA, AIP Conf. Proc. **1741**, 020002 (2016).

[11] Y. Ivanyushenkov, K. Harkay, M. Borland, R. Dejus, J. Dooling, C. Doose, L. Emery, J. Fuerst, J. Gagliano, Q. Hasse, M. Kasa, P. Kenesei, V. Sajaev, K. Schroeder, N. Sereno, S. Shastri, Y. Shiroyanagi, D. Skiadopoulos, M. Smith, X. Sun, E. Trakhtenberg, A. Xiao, A. Zholents, and E. Gluskin, Development and operating experience of a 1.1-m-long superconducting undulator at the Advanced Photon Source, Phys. Rev. Accel. Beams **20**, 100701 (2017).

[12] M. Kasa, E. Anliker, Q. Hasse, H. Hu, I. Kesgin, E. Moog, Y. Shiroyanagi, and Y. Ivanyushenkov, Design fabrication and testing of a 1.9-m-long 16.5-mm period NbTi superconducting undulator for the Advanced Photon Source Upgrade, IEEE Trans. Appl. Supercond. **32**, 1 (2022).

[13] Z. Chen, X. Yang, J. Wei, X. Zhang, X. Bian, Y. Li, and P. He, Vertical measurement and on-line correction of the magnetic field for a 1.5-m-long superconducting undulator, Nucl. Instrum. Methods Phys. Res., Sect. A **1047**, 167826 (2023).

[14] R. P. Walker, Phase errors and their effect on undulator radiation properties, Phys. Rev. ST Accel. Beams **16**, 010704 (2013).

[15] T. Tanaka, Universal representation of undulator phase errors, Phys. Rev. Accel. Beams **21**, 110704 (2018).

[16] C. Doose, M. Kasa, and S. Kim, End-field analysis and implementation of correction coils for a short-period NbTi superconducting undulator, in *Proceedings of 2011 Particle Accelerator Conference, New York, NY, USA* (2011), https://accelconf.web.cern.ch/PAC2011/papers/tup241.pdf.